Gaseous elemental mercury (GEM) response from sediment-covered, volcanogenic massive sulphide mineralization on southern Vancouver Island

Alexei S. Rukhlov[1, a], Nikolay R. Mashyanov[2], Pavel V. Pitirimov[3], Adrian S. Hickin[1], Maksym Golovetskyy[1], and Ben Coats[1]

[1] British Columbia Geological Survey, Ministry of Energy, Mines and Low Carbon Innovation, Victoria, BC, V8W 9N3
[2] Lumex-marketing LLC, 1 lit. B, Obruchevykh Street, St. Petersburg, 195220, Russia
[3] Lumex Instruments, Mission, BC, V4S 0A3
[a] corresponding author: Alexei.Rukhlov@gov.bc.ca

Recommended citation: Rukhlov, A.S., Mashyanov, N.R., Pitirimov, P.V., Hickin, A.S., Golovetskyy, M., and Coats, B., 2022. Gaseous elemental mercury (GEM) response from sediment-covered, volcanogenic massive sulphide mineralization on southern Vancouver Island. British Columbia Ministry of Energy, Mines and Low Carbon Innovation, British Columbia Geological Survey Paper 2022-01, pp. 123-135.

Abstract

New data from the Lara-Coronation polymetallic occurrence, southern Vancouver Island confirm that direct and continuous analysis of gaseous elemental mercury (GEM) concentrations in near-surface air using a portable RA-915M Zeeman Hg analyzer can map sediment-covered mineralization in real time. Detailed surveys across steeply dipping, massive sulphide zones in volcanic rocks of the McLaughlin Ridge Formation (Sicker Group; Middle to Late Devonian) confirm GEM haloes in near-surface air above the mineralization. Measured GEM concentrations range from 0.61 to 251 ng·m^{-3} in this study, with the strongest halo (206x background Hg) above exposed mineralization. Weak haloes (1.7x background Hg) mark sediment-covered mineralized zones. Simultaneously measured meteorological and in situ soil parameters appear to have no effect on measured GEM concentrations. Before sampling GEM above overburden, we disturbed surface sediment mechanically with a hoe. To model this method, we conducted experiments that measured GEM concentrations in the air of jars containing non-Hg ore minerals. These experiments suggest that elevated concentrations in Hg haloes reflect mechanically induced release of Hg^0 adsorbed in soils and vegetation. Real-time grid sampling of near-surface air reveals a pattern of northwest-trending GEM haloes reflecting bedrock structure, including a 224 by 30 m halo above the polymetallic VMS Coronation zone, covered by up to 22 m of overburden. This study confirms that the real-time GEM sampling of near-surface air can instantly delineate mineralized zones that are buried beneath overburden 10s of m thick. Real-time GEM sampling is a simple and effective technique for mineral exploration in overburden-covered areas.

Keywords: Gaseous elemental mercury (GEM), near-surface air, real-time survey, portable Lumex RA-915M Hg analyzer, ore minerals, bornite, galena, molybdenite, native copper, native silver, sphalerite, volcanic rocks, Sicker Group, Devonian, sediment-covered Lara-Coronation polymetallic occurrence, volcanogenic massive sulphide (VMS) mineralization, overburden, glacial deposits, mineral exploration under cover, southern Vancouver Island

1. Introduction

Mineral exploration in overburden-covered areas requires effective techniques such as atmochemical methods that sample highly mobile volatiles (e.g., CO_2, SO_2, He, Rn, and Hg), which form haloes in soil gas and near-surface atmosphere directly above mineral deposits (see Rukhlov et al., 2021b for an overview). Among atmochemical exploration methods, Hg vapour or gaseous elemental mercury (GEM) surveys are particularly informative (e.g., Fursov, 2006). This is because Hg is: 1) highly mobile (exists mostly as GEM); 2) common in many ore deposits (Babkin et al., 1976); and 3) a trace metal, with the very low background abundance in the Earth's crust of 45 ppb (Saukov et al., 1972; Rudnick and Gao, 2005) and ultra-low background concentrations in the atmosphere (<1.5 ng·m^{-3}; Sprovieri et al., 2016).

Modern GEM surveys use passive air sampling (e.g., McLagan et al., 2016; Jeon et al., 2020) or direct analysis of GEM concentrations in soil gas or air (e.g., Sun et al., 2017; Rukhlov et al., 2021b; Cabassi et al., 2022). Rukhlov et al. (2021b) reported GEM haloes in near-surface air at the sediment-covered, polymetallic Lara-Coronation occurrence, southern Vancouver Island (Fig. 1 inset). In the present study, we follow up this reconnaissance with detailed surveys across the mineralized zone at Lara-Coronation. We measured GEM concentrations in air 1 cm above ground in real time using a portable RA-915M Zeeman Hg analyzer, and simultaneously measured meteorological and in situ soil parameters. To minimize GEM removal and dilution due to wind and turbulent air movement, we sampled near-surface air under a bucket (cf. Rukhlov et al., 2021b). We performed experiments measuring GEM concentrations in the air of sealed glass jars containing samples of selected ore minerals to model the instant release of GEM adsorbed in overburden at superimposed Hg haloes in response to mechanical disturbance. Our study

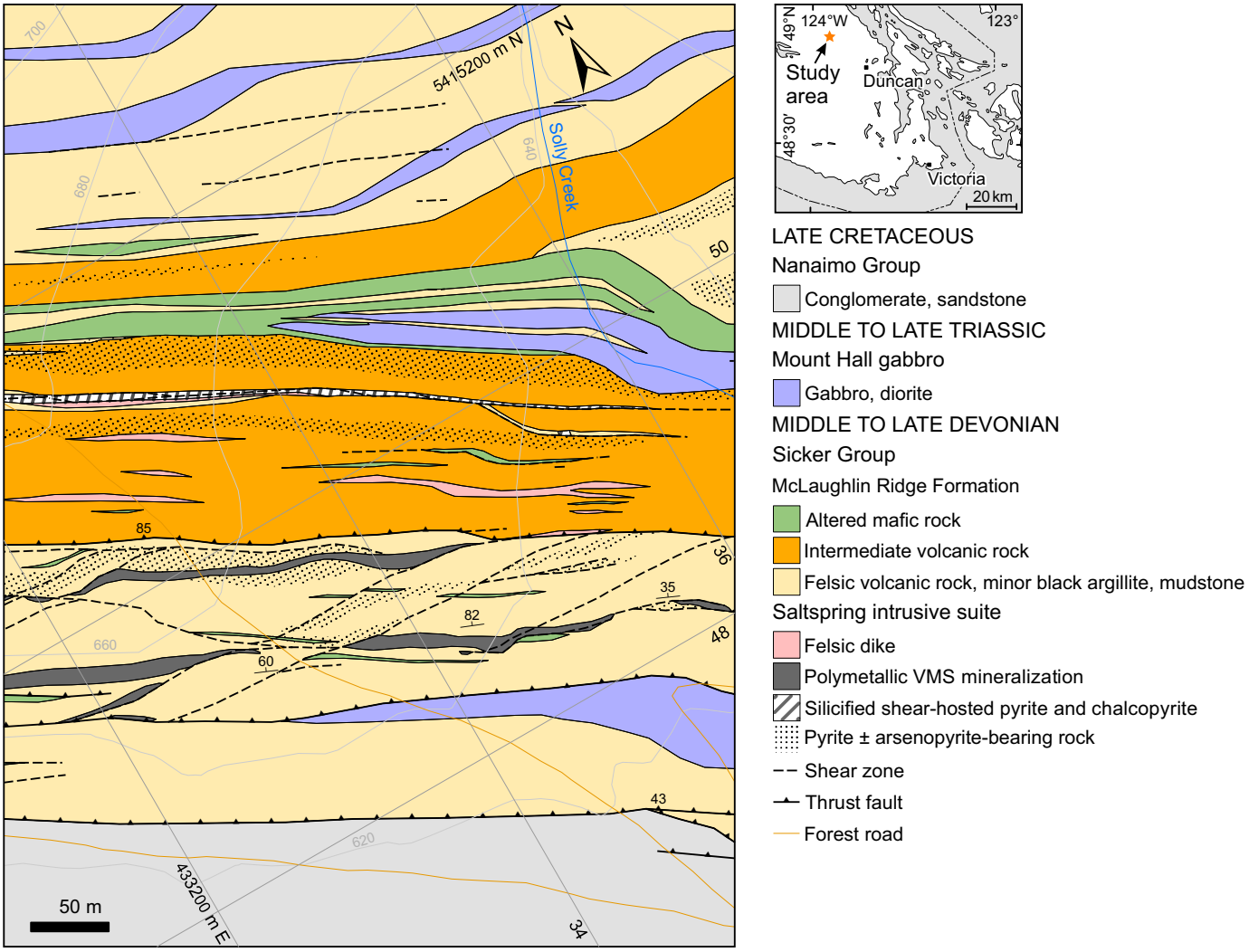

Fig. 1. Location (inset) and geology of the Lara-Coronation occurrence; NAD 83, UTM zone 10. Geology after Muller (1977), Kapusta et al. (1988), Massey et al. (1991), Massey (1995), Wetherup (2010), Ruks (2015), and Bodnar (2017).

confirms that simple, real-time GEM sampling of near-surface air can instantly map mineralized zones covered by overburden 10s of m thick.

2. Geological setting, Lara-Coronation polymetallic volcanogenic massive sulphide occurrence

The Lara-Coronation volcanogenic massive sulphide (VMS) Zn-Cu-Pb-Ag-Au occurrence (MINFILE 092B 129) is about 15 km northwest of Duncan, in the traditional lands of the Hul'qumi'num and Snuneymuxw First Nations, southern Vancouver Island (Fig. 1). The area is mostly covered by up to 30 m of glacial sediments (Kapusta et al., 1988; Bodnar, 2017). The polymetallic mineralization (Coronation zone) comprises lenses (up to 16 m thick) of banded and massive sphalerite, pyrite, chalcopyrite, and galena with minor tetrahedrite, tennantite, bornite, electrum, pearceite, and arsenopyrite. Associated mineralization includes chalcopyrite-pyrite stringers in silicified shear zones and pyrite-rich horizons (Northcote and Muller, 1972; Kapusta et al., 1988; Kelso and Wetherup, 2008; Wetherup, 2010; Ruks, 2015; Bodnar, 2017). Host rocks are greenschist-facies, sheared and silicified, felsic and intermediate volcanic rocks of the McLaughlin Ridge Formation (Sicker Group; Middle to Late Devonian), which dip steeply northeast. Coeval felsic intrusions of the Saltspring plutonic suite and mafic to intermediate intrusions of the Mount Hall gabbro (Middle to Late Triassic) cut the volcanic rocks. Folded and imbricated by thrust faults, the older rocks are juxtaposed against siliciclastic rocks of the Nanaimo Group (Late Cretaceous) along a northwest-trending fault (Muller, 1977; Kapusta et al., 1988; Masey et al., 1991; Massey, 1995; Wetherup, 2010; Ruks, 2015; Bodnar, 2017).

3. Methods

Real-time GEM mass concentrations (in $ng \cdot m^{-3}$) in near-surface air were directly and continuously measured using a portable Lumex RA-915M Zeeman Hg analyzer during foot

traversing at the Lara-Coronation occurrence. The instrument has a concentration detection range of 0.5 to 20,000 ng·m^{-3} and a response time of one second. Baseline (zero Hg signal) was automatically measured for 60 seconds every 2 to 3 minutes using a built-in, high-efficiency (>98%) sorption filter. The relative intrinsic error of the measurement is less than ±20%. GEM concentrations were automatically corrected for drift and normalized to standard temperature (20°C) and pressure (101.3 kPa). We used the average of 60 or 120 readings (1 second each) per station, which were automatically processed by a Lumex RAPID software running on a pocket PC connected to the instrument in the field. Stations were spaced 4 to 36 m along traverses (260 to 500 m long; Table 1). We sampled air at 1 cm above ground via a probe attached to the instrument's air intake inlet with a built-in dust filter (Fig. 2). The probe consists of: 1) a 1.3 m hose (2 cm diameter); 2) a dust filter (6.4 cm diameter housing; 5.1 cm diameter insert) with barb connectors and an intake tube (23 cm long; 8 mm diameter); 3) a 4.2 L bucket (21 cm diameter) with a fitting through bottom for the intake tube; and 4) a stick holding the bucket and about one third of the hose secured with tape (Fig. 3). The distance between the end of the tube inside the bucket and ground (the air sampling height) was set to approximately 1 cm. In contrast to Rukhlov et al. (2021b), we sampled the air under the bucket to minimize wind influence on GEM concentration (Yasutake et al., 2011).

Fig. 2. Measuring real-time gaseous elemental mercury (GEM) in air 1 cm above ground.

Fig. 3. Air probe.

A chopstick attached to the edge of the bucket creates a small gap when the probe is placed against the ground, which is necessary to maintain the analyzed air flow of 10 L·min^{-1}.

We performed five orientation surveys along two southwest-northeast profiles (A′-A and B′-B; Figs. 4, 5) across the known mineralized zones to determine optimal parameters. GEM concentrations in near-surface air were measured: 1) without mechanical disturbance of the surface before sampling; and 2) immediately after punching several times or partly removing the top 5-15 cm layer across an area ca. 20 cm in diameter with the pointed edge of an Estwing GP100 hoe pick (Fig. 6). The shorter measurements (1 min per station), coupled with mechanically agitated surface immediately before sampling, yielded the strongest GEM haloes above the known mineralization (Table 1). We adopted these parameters for an areal survey, following a grid of 5 lines (450 m long each; 50 m spacing), with stations every 13 to 36 m along the lines.

To model mechanically induced release of volatile Hg^0 adsorbed in overburden, we measured GEM concentrations in the air of sealed glass jars (1 L) containing samples of sphalerite, galena, molybdenite, bornite, and native metals (Table 2). Air was sampled via a hose with a dust filter 1 cm above samples: 1) after several days of undisturbed storage in closed jars, and 2) two to five minutes after gently shaking the samples in re-closed jars. The GEM concentrations in air were continuously measured until a plateau concentration in terms of time (s) vs. GEM (ng·m^{-3}), with 55 to 108 readings (1 second each) acquired per run. We also measured air 1 m above ground in Victoria, B.C. (total 3 runs; 80 seconds each) to check the background GEM concentrations between 3 to 6 runs of air above the samples of ore minerals.

Air temperature, relative humidity, barometric pressure, wind speed, and wind direction (azimuth) were simultaneously measured every 5 seconds using a Kestrel 5500 meter mounted on a tripod under umbrella at a fixed location in the study area (Fig. 7). We used a Garmin Glo 2 GPS-GLONASS to acquire coordinates every 2 seconds. In-situ soil parameters (temperature, moisture content, electrical conductivity, and pH) were measured at stations along profile 1 (A′-A) simultaneously with the first GEM orientation on July 15, 2021 (Table 1). We used an Extech 39240 thermometer with a 7 cm long stainless-steel probe; an Extech MO750 soil moisture meter with a

Table 1. Summary of GEM surveys in air 1 cm above ground at the Lara-Coronation polymetallic occurrence.

Survey		Sampling site		GEM data[1]		Meteorological parameters[2]						GEM halo	
Date	**Time**	**Spacing**	**Surface[3]**	**Readings**	**Baseline**	**T (°C)**	**RH (%)**	**P_0 (mb)**	**Wind (m·s^{-1})**	**Azimuth**	**Weather**	**Contrast[4]**	**Extent (m)[5]**
Profile 1 (A'-A; 260 m) across mineralization exposed in an old exploration trench (2020 GEM anomaly); overburden thickness varies from 0 to 18 m.													
15.07.2021	12:01 to 14:48	4 to 25 m	Undisturbed	120	60 s, every 3 min	19.2 to 26.3	39.4 to 52.2	1019.7 to 1020.4	0 to 5.6	160 to 190	Sunny	3.5	20
	15:09 to 15:52	4 to 25 m	Undisturbed	60	60 s, every 2 min	20.0 to 25.6	37.9 to 47.2	1019.7 to 1020.0	0 to 4.9	150 to 180	Few clouds	6.0	20
20.07.2021	11:55 to 12:38	4 to 25 m	Agitated	60	60 s, every 2 min	18.8 to 23.4	31.6 to 41.3	1024.5 to 1024.6	0 to 4.3	290 to 300	Few clouds	206	29
Profile 2 (B'-B; 500 m) across sediment-covered mineralization (2020 GEM anomaly); overburden thickness varies from 5 to 17 m.													
20.07.2021	13:20 to 14:27	6 to 25 m	Undisturbed	60	60 s, every 2 min	19.4 to 24.6	29.2 to 39.1	1024.1 to 1024.5	0 to 5.4	280 to 340	Few clouds	1.4	22
	15:10 to 16:17	4 to 33 m	Agitated	60	60 s, every 2 min	20.0 to 24.1	29.8 to 39.5	1023.5 to 1024.0	0 to 4.4	280 to 340	Few clouds	1.7	25
Grid of 5 x 450 m lines (50 m spacing); overburden thickness varies from <1 to 22 m.													
21.07.2021	11:01 to 14:55	13 to 36 m	Agitated	60	60 s, every 2 min	14.5 to 22.0	37.8 to 49.1	1023.4 to 1024.3	0 to 6.5	280 to 70	Few clouds	1.7	224 x 30[6]

[1] Real-time, gaseous elemental mercury (GEM) mass concentrations (one reading per second; 60 or 120 readings per site); baseline (zero Hg signal) measured for 60 seconds every 2 to 3 minutes.
[2] Meteorological parameters every 5 seconds: **T**- air temperature (°C); **RH** - relative humidity (%); **P_0** - barometric pressure (mb); **Wind** - wind speed (m·s^{-1}); **Azimuth** – predominant wind direction.
[3] **Undisturbed** – no intentional agitation of surface immediately before measuring GEM; **Agitated** - top 5 to 15 cm surface layer disturbed with a hoe pick immediately before measuring GEM.
[4] Ratio of the mean GEM concentration (based on 60 or 120 measurements per site) in near-surface air above a known mineralized zone to the median GEM concentration of the survey.
[5] Width of a GEM (ng·m^{-3}) peak above a known mineralized zone on profile (see Fig. 5).
[6] Footprint of a GEM halo in near-surface air above the polymetallic Coronation zone (volcanogenic massive sulphide; see Fig. 4).

20 cm long, heavy-duty probe; a Hanna HI98331 direct soil EC tester with an 11.4 cm long, stainless-steel probe; and a Hanna HI99121 direct soil pH meter with a glass electrode. The single-junction pH electrode was calibrated using pH 4.01 and 7.00 buffers on the same day. We used a conical plastic auger to perforate dry soil 3 to 4 cm deep and a few mL of deionized water added to the borehole before inserting the pH sensor. The equipment was carefully rinsed with deionized water after each measurement.

4. Results

The complete dataset upon which the following is summarized is presented in Rukhlov et al. (2021a). The GEM surveys at the Lara-Coronation VMS Zn-Cu-Pb-Ag-Au occurrence (MINFILE 092B 129) include orientation profiles performed on July 15, 2021 and July 20, 2021 and a grid survey performed on July 21, 2021 (Fig. 4). Table 1 provides a summary of the surveys, GEM haloes, and simultaneously measured meteorological parameters. Table 2 provides a statistical summary of the real-time GEM data for air sampled at 1 cm above ground at the Lara-Coronation occurrence; air 1 m above ground in Victoria, B.C.; and air of sealed glass jars containing selected ore minerals.

4.1. GEM in near-surface air

We carried out surveys along the southwest-northeast traverses (030° azimuth; 260 to 500 m long) on a clearcut across polymetallic mineralization at the Coronation zone, covered by up to 22 m of glacial sediments (Fig. 4; Kapusta et al., 1988; Bodnar, 2017). Profile 1 (A′-A; 260 m) is across the main mineralized zone exposed in an overgrown, partly flooded exploration pit trenched in approximately 1986. Profile 2 (B′-B; 500 m) is across the same zone, 230 m along strike to the northwest, where mineralization is covered by at least 17 m of glacial sediments (Fig. 4). Weather conditions (sunny to a mix of sun and clouds) were generally consistent for all surveys. Air temperature varied between 14.5 and 26.3°C, relative humidity between 29.2 and 52.2%, and barometric pressure between 1019.7 and 1024.6 mb. Predominantly southerly winds (150 to 190° azimuth) with gusts up to 5.6 $m \cdot s^{-1}$ on July 15, 2021 became predominantly west and east (280 to 070° azimuth), with gusts up to 6.5 $m \cdot s^{-1}$ on July 20 and 21 (Table 1).

Measured GEM concentrations (the average of 60 or 120 values per point) in air 1 cm above ground at the Lara-Coronation occurrence range from 0.61 to 251 $ng \cdot m^{-3}$, averaging 2.37 ±16.4 $ng \cdot m^{-3}$ (n=231; Table 2). The strongest GEM halo marks exposed massive sulphide mineralization containing up to 90 ppm Hg in the trench (Kelso and Wetherup, 2008; Bodnar, 2017). The median value of 1.13 $ng \cdot m^{-3}$ is consistent with the average GEM concentration (background) in air 1 m above ground in Victoria, B.C. (1.03 ±0.32 $ng \cdot m^{-3}$; n=240; based on 3 runs, 80 s each), and with the median GEM concentration in near-surface air for southern Vancouver Island (1.40 $ng \cdot m^{-3}$; n=9660; based on the average of 10 values per point; Rukhlov et al., 2021b).

Orientation surveys in this study confirm the anomalous GEM haloes in near-surface air at Lara-Coronation (Fig. 5; Rukhlov et al. 2021b). GEM concentrations, measured without mechanical disturbance of surface materials immediately before sampling, range from 0.79 to 5.86 $ng \cdot m^{-3}$, with the median (background) value of 1.05 $ng \cdot m^{-3}$ (n=75; Table 2). The shorter measurements (1 min per site) yielded a slightly stronger GEM halo (6.0x background Hg) than the longer measurements (2 min per site; 3.5x background Hg; Table 1; Fig. 5a). In contrast, GEM concentrations in near-surface air, measured immediately after mechanically agitating the top 5 to 15 cm surface layer, range from 0.61 to 251 $ng \cdot m^{-3}$, with the median (background) value of 1.21 $ng \cdot m^{-3}$ (n=156; Table 2). Therefore, the effect of mechanically disturbing a site before sampling yields a GEM response that is two orders of magnitude stronger (206x background Hg) relative to the undisturbed surface at the same location (Table 1; Fig. 5). Regardless of bedrock, GEM concentrations in near-surface air away from the mineralized zone along profile 1 are generally <2 $ng \cdot m^{-3}$ (i.e. background-level), consistent with the low Clarke value for the Earth's crust (45 ppb Hg; Saukov et al., 1972; Rudnick and Gao, 2005) and with generally uniform Hg abundances in different rock types away from Hg anomalies (Fursov, 2006). An anomalous GEM halo (3.16 $ng \cdot m^{-3}$) also marks a steep fault covered by 8 m of overburden at about 125 m along section A′-A (Rukhlov et al., 2021b; Fig. 5a).

Orientation surveys along profile 2 (B′-B; Fig. 4) revealed background-level GEM variations (up to 1.7x background Hg) above the mineralization covered by at least 17 m of clay-bearing glacial sediments (Fig. 5b). GEM concentrations in near-surface air, measured above mechanically disturbed materials (0.89 to 2.23 $ng \cdot m^{-3}$, averaging 1.37 ±0.34 $ng \cdot m^{-3}$; n=34), are slightly higher than those above undisturbed surfaces (0.83 to 1.44 $ng \cdot m^{-3}$, averaging 1.08 ±0.14 $ng \cdot m^{-3}$; n=33). A GEM spike at about 300 m along the profile marks a silicified shear zone with pyrite-chalcopyrite stringers (Rukhlov et al., 2021b), but spikes at about 50 m, 250 m, and between 350 and 450 m along the profile do not correspond to known mineralization (Fig. 5b). An extensive GEM halo (100 m wide) near the northeastern end of the profile is above felsic volcanic rocks of the McLaughlin Ridge Formation (Sicker Group), which host the Coronation zone, 200 m to the southwest, and several other polymetallic zones in the area (Kapusta et al., 1988; Kelso and Wetherup, 2008; Ruks, 2015; Bodnar, 2017). Previous multi-media geochemical surveys at Lara revealed a Hg aureole at Lara-Coronation, with up to 460 ppb Hg in soils and up to 133 ppb Hg in vegetation, reflecting the massive sulphide mineralization (Kapusta et al., 1988; Kelso and Wetherup, 2008; Bodnar, 2017; Heberlein et al., 2017). Elevated Hg contents in soils and vegetation correlate with the GEM halo near the northeastern end of B′-B, which may indicate an unknown mineralized zone (Fig. 5b).

Based on the orientation surveys, we consider that the optimal survey parameters include mechanically disturbing surface materials immediately before measurements are taken

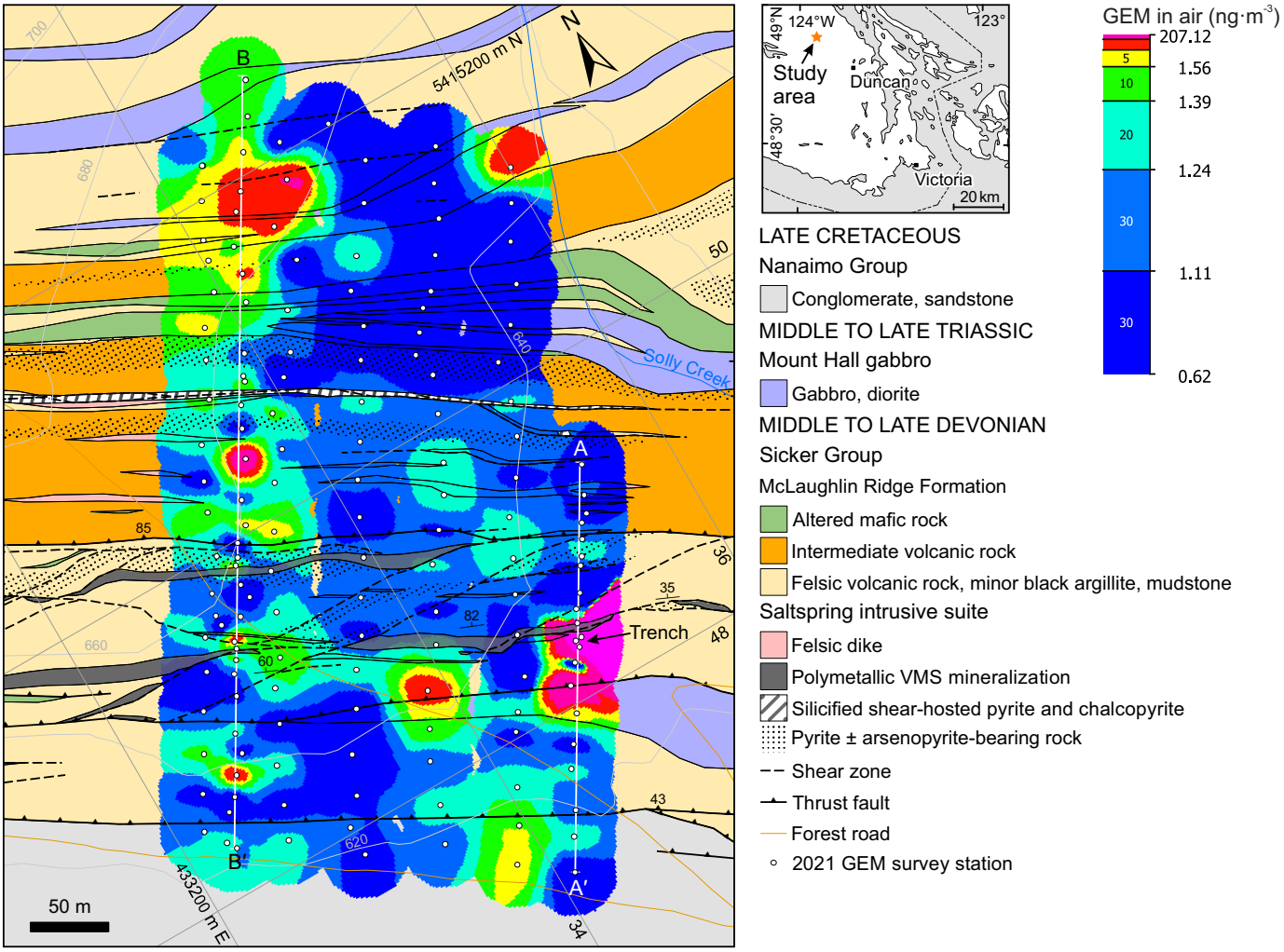

Fig. 4. Percentile-gridded, real-time GEM concentrations (ng·m^{-3}) in air 1 cm above ground and position of section lines A′-A and B′-B. Gridding interpolation based on modified inverse distance weighting method.

and briefer measurement times (1 minute per site). We adopted these parameters for a grid survey at Lara-Coronation on July 21, 2021. GEM concentrations measured every 13 to 36 m along 5 southwest-northeast traverses (030° azimuth; 450 m long each; 50 m spacing) range from 0.61 to 1.98 ng·m^{-3}, averaging 1.21 ±0.24 ng·m^{-3} (n=101). GEM response from the sediment-covered polymetallic mineralization is 1.7x background Hg, consistent with the orientation results discussed above (Table 1). Combined with the orientation data for mechanically disturbed sites, the percentile-gridded, real-time GEM values reveal a 224 by 30 m halo above the Coronation zone (Fig. 4). Weak haloes also trace the silicified shear zone with sulphide stringers at 300 m along B′-B for at least 220 m along strike. The prominent halo in the northern corner of the grid discussed above extends both to the southeast and northwest (open), with a footprint of at least 100 by 60 m. Except for a lone anomaly above felsic volcanic rocks in the eastern corner of the grid, background GEM concentrations characterize much of the area immediately west of Solly Creek (Fig. 4). On the other hand, GEM anomalies are more common to the west, within a band along B′-B at least 50 m wide. Notably, a pattern of northwest-trending GEM haloes emerges that reflects the bedrock structure (Fig. 4).

4.2. Experiment to investigate mechanically induced release of GEM

Surveys using mechanical agitation of surface materials immediately before sampling yielded up to two orders of magnitude stronger GEM anomalies (see above). The effect of mechanically induced emission of adsorbed Hg^0 is well known from soil-gas surveys (e.g., Zherebtsov et al., 1992) and is the basis for GEM-monitoring of Neotectonic activity and other geohazards such as landslides (e.g., Stepanov, 1997; Sun et al., 2017).

To investigate the release of GEM from mechanically disturbed overburden, we performed experiments measuring GEM concentrations in the air of glass jars (1 L) containing samples of ore minerals such as sphalerite, galena, molybdenite,

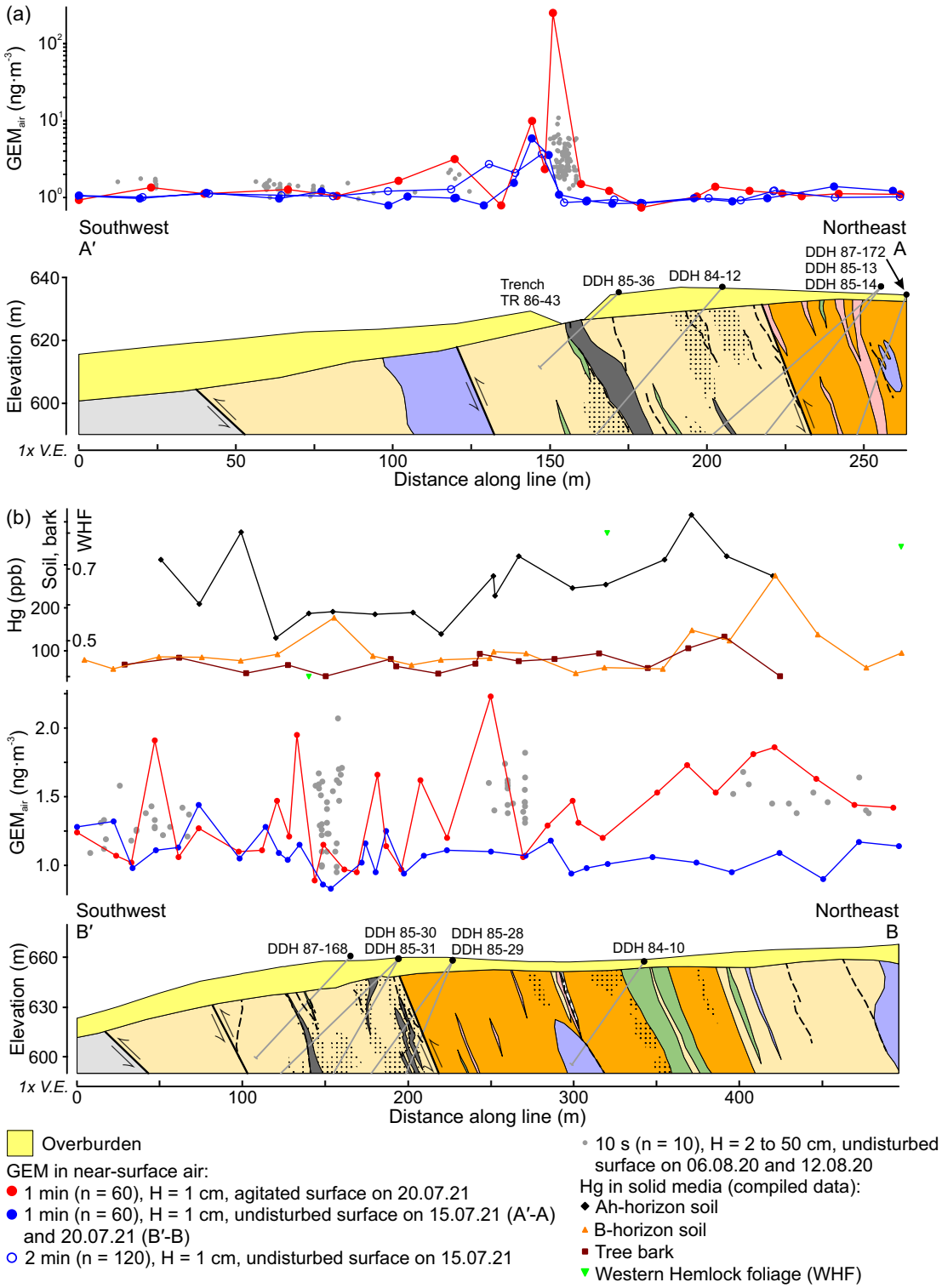

Fig. 5. Mercury concentrations with respect to distance along line (m) and cross-sections at the Lara-Coronation occurrence (see Fig. 4). Overburden thickness from Kapusta et al. (1988) and Bodnar (2017); diamond drill hole (DDH) collar locations and paths from Kapusta et al. (1988); geology legend as in Figure 4. H-sampling height above ground; n-number of GEM measurements (one per second) per site; grey symbols-mean GEM concentrations in air 2 to 50 cm above ground on August 6, 2020 and August 12, 2020 (from Rukhlov et al., 2021b). **a)** Profile 1 showing mean GEM (ng·m^{-3}; note the logarithmic scale) in air 1 cm above ground on July 15, 2021 (undisturbed surface; blue symbols) and on July 20, 2021 (agitated surface; red symbols) and southwest-northeast cross-section A′-A (1x vertical exaggeration). **b**) Profile 2 showing Hg (ppm) in soil and vegetation and mean GEM (ng·m^{-3}) in air 1 cm above ground on July 20, 2021 (symbols as in a), and southwest-northeast cross-section B′-B (1x vertical exaggeration). Soil and vegetation geochemical data compiled from Bodnar (2017) and Heberlein et al. (2017).

Fig. 6. Sediment surface mechanically disturbed using an Estwing GP100 hoe pick immediately before measuring GEM concentration.

Fig. 7. Measuring air temperature, barometric pressure, relative humidity, wind speed, and wind direction (azimuth) simultaneously with the GEM concentrations.

bornite, native copper, and native silver (Table 2). Even though these are non-Hg minerals, they contain trace amounts of Hg (0.15 to 92.2 ppm), directly measured by thermal decomposition of small splits of the samples (34 to 103 mg) using a Lumex RA-915 Lab analyzer in this study. Having stored the samples undisturbed in closed jars with screw lids for several days, the jars were opened immediately before sampling air 1 cm above the samples for 70 to 93 seconds, until the real-time GEM concentration reached a plateau in terms of time (s) vs. GEM ($ng \cdot m^{-3}$; Fig. 8). The jars were re-closed and gently shaken, and the air was reanalyzed 2 to 5 minutes after shaking. We measured GEM concentrations in air 1 m above ground in Victoria to check the background GEM concentrations after every 3 to 6 runs. The consistent background GEM concentrations rule out any Hg settling on the instrument's communications during the analysis (Table 2).

Running one-second GEM values in undisturbed jars ranged from <0.5 (the instrument's detection limit) to 274 $ng \cdot m^{-3}$ (n=549; Table 2). Time (s) vs. GEM ($ng \cdot m^{-3}$) profiles for all but one sample had a peak at about 10 seconds, with native silver (89 g) and galena (246 g) showing the maximum GEM concentrations (Fig. 8). Jars with molybdenite, sphalerite, native copper, and coarse-grained galena (54 g) had lower, but still anomalous GEM concentrations. Bornite (75 g), on the other hand, showed no peak, with background-level GEM concentrations up to 2.4 $ng \cdot m^{-3}$ (Fig. 8f; Table 2). The plateau-level GEM concentrations at the end of the first run (undisturbed samples) for all samples ranged from 1.53 to 11.4 $ng \cdot m^{-3}$, based on the median values (Table 2). The running one-second GEM values in the air of the shaken jars ranged from <0.5 to 124 $ng \cdot m^{-3}$ (n=502; Table 2). Time (s) vs. GEM ($ng \cdot m^{-3}$) profiles of the shaken samples are generally like those of undisturbed samples, having peak concentrations at 10 seconds, but show different sample vs. maximum GEM ($ng \cdot m^{-3}$) relationships. In contrast to GEM released from samples undisturbed for several days, native copper yielded almost 4x higher GEM concentration (124 $ng \cdot m^{-3}$) five minutes after shaking (Fig. 8c). Sphalerite and coarse-grained galena show similar levels of GEM before and after shaking, but a fragment of a large galena crystal (246 g), native silver, and molybdenite yielded 2 to 16x lower GEM levels after shaking relative to those released from the samples after undisturbed storage for several days (Table 2; Fig. 8). GEM concentrations (up to 1.6 $ng \cdot m^{-3}$) in a jar with bornite after shaking were indistinguishable from background GEM in air (Fig. 8f).

In summary, our experiments confirm release of adsorbed Hg at superimposed haloes when measurements were taken after surface materials at sample sites were mechanically disturbed. That the non-Hg ore minerals "exhale" Hg underlines the usefulness of GEM surveys in exploring for diverse deposits (Fursov, 2006).

4.3. Meteorological measurements

Seasonal and diurnal changes in meteorological conditions can influence GEM emission (see discussion in Rukhlov et al., 2021b). In contrast to Rukhlov et al. (2021b), measured GEM concentrations in this study do not show any effects of meteorological parameters, which were simultaneously measured (Fig. 9).

Table 2. Statistical summary of GEM concentrations in air 1 cm above ground and air of jars containing selected ore minerals.

Analysis	Run[1]	N	n	GEM concentrations in air (ng·m^{-3})									
				Mean	σ	Minimum	Percentiles						Maximum
							25	50	80	90	95	98	99	
Air 1 cm above ground at the Lara-Coronation polymetallic occurrence														
Undisturbed surface	na	75	na	1.23	0.73	0.79	0.97	1.05	1.22	1.41	2.89	4.73	5.86	5.86
Agitated surface	na	156	na	2.91	20.0	0.61	1.06	1.21	1.49	1.65	1.92	3.05	114	251
All data	na	231	na	2.37	16.4	0.61	1.02	1.13	1.41	1.64	1.96	3.61	8.60	251
Air 1 m above ground in Victoria, B.C.														
Background		na	240	1.03	0.32	0.05	0.83	1.02	1.29	1.48	1.60	1.66	1.77	1.82
Air 1 cm above samples of selected ore minerals in sealed glass jars														
Sphalerite (ZnS), coarse-grained aggregate; 47 g	1	na	70	12.1	13.9	0.58	4.90	7.71	14.8	31.8	52.6	64.8	66.6	66.6
	2	na	65	8.44	12.7	0.52	2.59	3.28	8.68	29.7	47.3	53.4	54.9	54.9
Galena (PbS), fragment of a large crystal; 246 g	1	na	72	26.1	48.6	0.76	3.32	3.94	39.0	92.4	161	212	225	225
	2	na	61	2.85	2.88	0.60	1.39	1.90	3.36	6.48	10.8	13.9	14.0	14.0
Native copper (Cu), dendritic aggregate; 24 g	1	na	93	5.63	3.89	0.36	4.26	4.88	5.99	7.16	12.8	23.5	26.7	26.7
	2	na	108	15.3	16.9	0.81	9.00	10.4	14.0	27.3	55.7	90.8	102	103
Native silver (Ag), dendritic aggregate; 89 g	1	na	93	27.5	51.9	0.74	9.71	11.4	13.5	68.2	180	258	274	274
	2	na	77	15.2	22.0	1.02	7.36	9.68	14.3	22.3	76.6	121	124	124
Molybdenite (MoS_2), single crystal; 18 g	1	na	71	9.12	19.8	0.69	1.38	1.86	5.76	28.1	64.6	94.2	94.7	94.7
	2	na	69	2.10	2.12	0.47	1.11	1.43	2.08	5.20	7.95	10.4	10.5	10.5
Bornite (Cu_5FeS_4), massive aggregate; 75 g	1	na	72	1.52	0.39	0.13	1.26	1.53	1.91	2.02	2.11	2.27	2.36	2.36
	2	na	55	0.94	0.34	0.18	0.68	0.96	1.26	1.37	1.48	1.62	1.63	1.63
Galena (PbS), coarse-grained aggregate; 54 g	1	na	78	2.73	0.91	0.50	2.25	2.69	3.43	3.88	4.56	4.93	4.99	4.99
	2	na	67	3.51	1.15	0.52	3.14	3.60	4.11	4.33	5.97	6.81	6.91	6.91

[1] Air of jars containing ore minerals: **1** - after several days of undisturbed storage; **2** - two to five minutes after gently shaking the sample.
N - number of mean values used to calculate the statistical parameters; **n** – number of one-second measurements used to calculate the statistical parameters for air in Victoria, B.C. and air of jars containing samples of ore minerals; **σ** - standard deviation.

4.4. In-situ soil parameters

Rukhlov et al. (2021b) attributed the variable intensity of GEM haloes at Lara-Coronation to changes in overburden moisture. To investigate the influence of soil conditions in the present study, we measured in situ soil (2 to 5 cm deep) temperature, moisture, electrical conductivity, and pH at 19 stations along profile A'-A, simultaneously with the GEM survey on July 15, 2021 (from 12:01 to 14:48; Table 1). Soil temperature ranged from 16.9 to 44.1°C (averaging 27.93 ±7.82°C), moisture content (humidity) from 0 to 16.4%, (averaging 1.70 ±4.35%), electrical conductivity (EC; in microsiemens per cm) from 0 to 178 µS·cm^{-1} (averaging 20.5 ±42.2 µS·cm^{-1}), and pH from 4.3 to 6.4 (averaging 5.38 ±0.65). Variations in soil temperature mainly reflect direct exposure to the sun. Because of persistent dry weather, detectable moisture in soil was measured only at: 119 m (7.9%), 131 m (8.0%), and 147 m (16.4%) along profile A′-A (Fig. 5a). The maximum moisture content coincides with the maximum EC and pH values, and the minimum temperature was measured in rusty mud near the bottom of the partly flooded trench with exposed mineralization.

In summary, in-situ soil moisture and electrical conductivity display a weak correlation with simultaneously measured GEM concentrations, but in-situ soil temperature and pH generally do not (Fig. 10). Because all surveys in this study were performed in consistently dry weather conditions, we could not evaluate the moisture effect.

5. Discussion: GEM haloes above mineralization

Detailed, real-time sampling of GEM in air 1 cm above ground in this study confirmed GEM haloes in near-surface atmosphere above sediment-covered, polymetallic mineralization at Lara-Coronation (Figs. 4, 5; Rukhlov et al., 2021b). Background-level GEM haloes mark mineralized zones covered by glacial sediments (up to 22 m thick; Fig. 5b). Figure 11 schematically illustrates Hg dispersal from a drift-covered ore deposit and the processes that form GEM haloes in soil gas and near-surface atmosphere. The ore and its primary and secondary haloes release highly mobile and chemically stable Hg^0 (i.e., GEM) via sublimation, reduction, electrochemical reactions, and biogenic oxidation in the supergene zone. Concentration, temperature, and pressure gradients drive the upward GEM flux by diffusion and filtration along permeable zones, thereby forming constantly renewed superimposed Hg haloes directly above the ore.

Rather than forming dispersal plumes, GEM haloes in near-surface atmosphere occur directly above deposits because

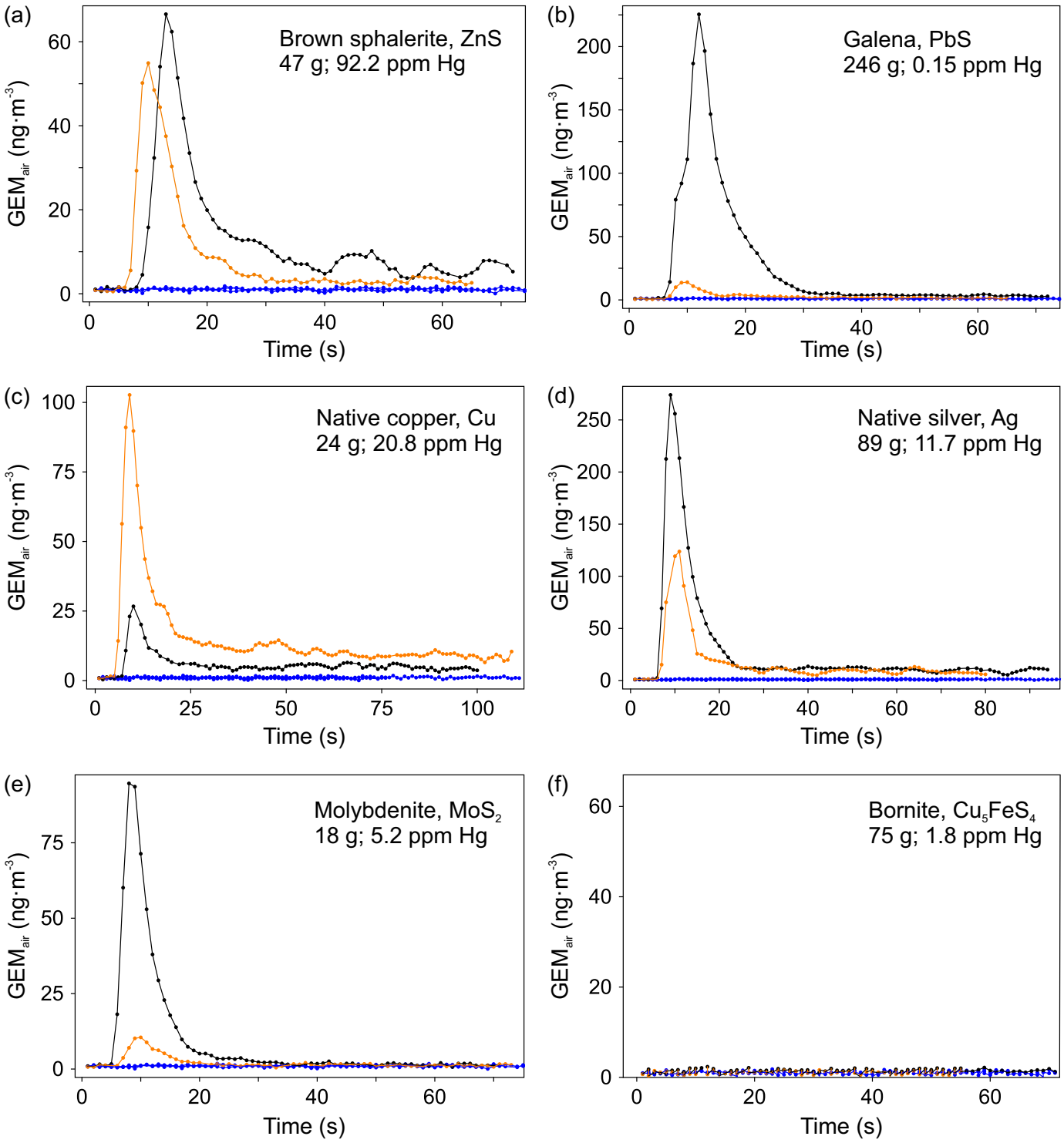

Fig. 8. Time (s) vs. GEM (ng·m^{-3}) in air 1 cm above samples of selected ore minerals in glass jars (1 L) after several days of undisturbed storage in closed jars (black symbols) and 2 to 5 min after the jars were re-sealed and gently shaken (orange symbols), and 1 m above ground in Victoria, B.C. (background GEM concentrations; blue symbols). **a)** Brown sphalerite, ZnS. **b)** Galena, PbS. **c)** Native copper, Cu. **d)** Native silver, Ag. **e)** Molybdenite, MoS_2. **f)** Bornite, Cu_5FeS_4. Total Hg concentrations in the samples (34 to 103 mg splits) of ore minerals directly measured by thermal decomposition using a Lumex RA-915Lab analyzer.

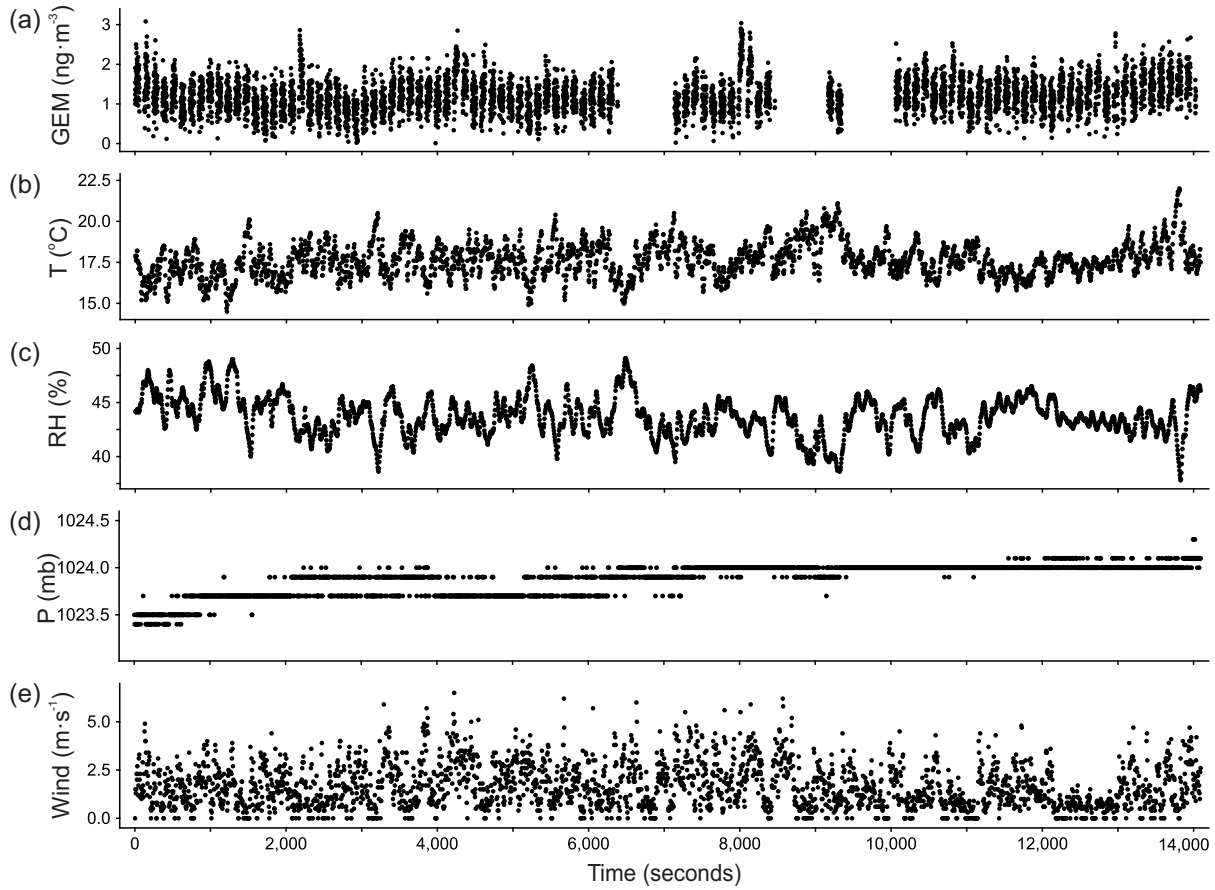

Fig. 9. Scatter plots of time (in seconds) vs. simultaneously measured, real-time GEM concentrations in near-surface air (GEM, in nanograms per cubic metre), air temperature (T, in degrees Celsius), relative humidity (RH, in %), barometric pressure at sea level (P, in millibars), and wind speed (Wind, in m per second) on July 21, 2021. **a)** Time (s) vs. GEM (ng·m^{-3}). **b)** Time (s) vs. T (°C). **c)** Time (s) vs. RH (%). **d)** Time (s) vs. P (mb). **e)** Time (s) vs. wind (m·s^{-1}).

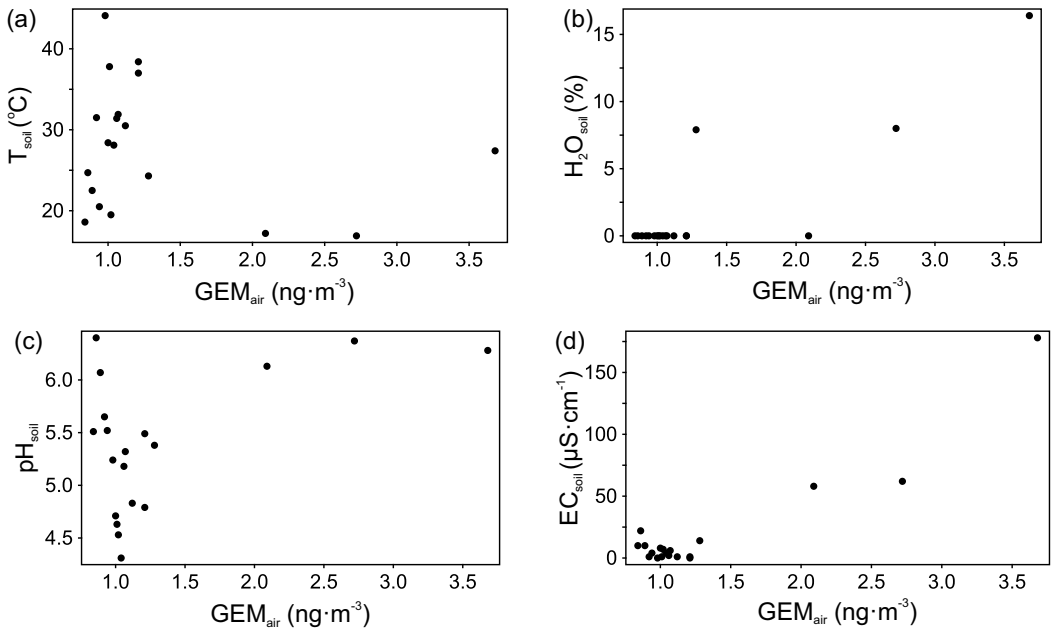

Fig. 10. Scatter plots of GEM concentrations in near-surface air (GEM_{air}, in nanograms per cubic metre) vs. in situ soil temperature (T_{soil}, in degrees Celsius); moisture content (H_2O_{soil}, %); hydrogen ion activity, defined as $-\log_{10}a(H^+)$, where $a(H^+)$ is the activity of the hydrogen ion (pH_{soil}); and electrical conductivity (EC_{soil}, in microsiemens per cm) for line A′-A) on July 15, 2021. **a)** GEM_{air} (ng·m^{-3}) vs. T_{soil} (°C). **b)** GEM_{air} (ng·m^{-3}) vs. H_2O_{soil} (%). **c)** GEM_{air} (ng·m^{-3}) vs. pH_{soil}. **d)** GEM_{air} (ng·m^{-3}) vs. EC_{soil} (µS·cm^{-1}).

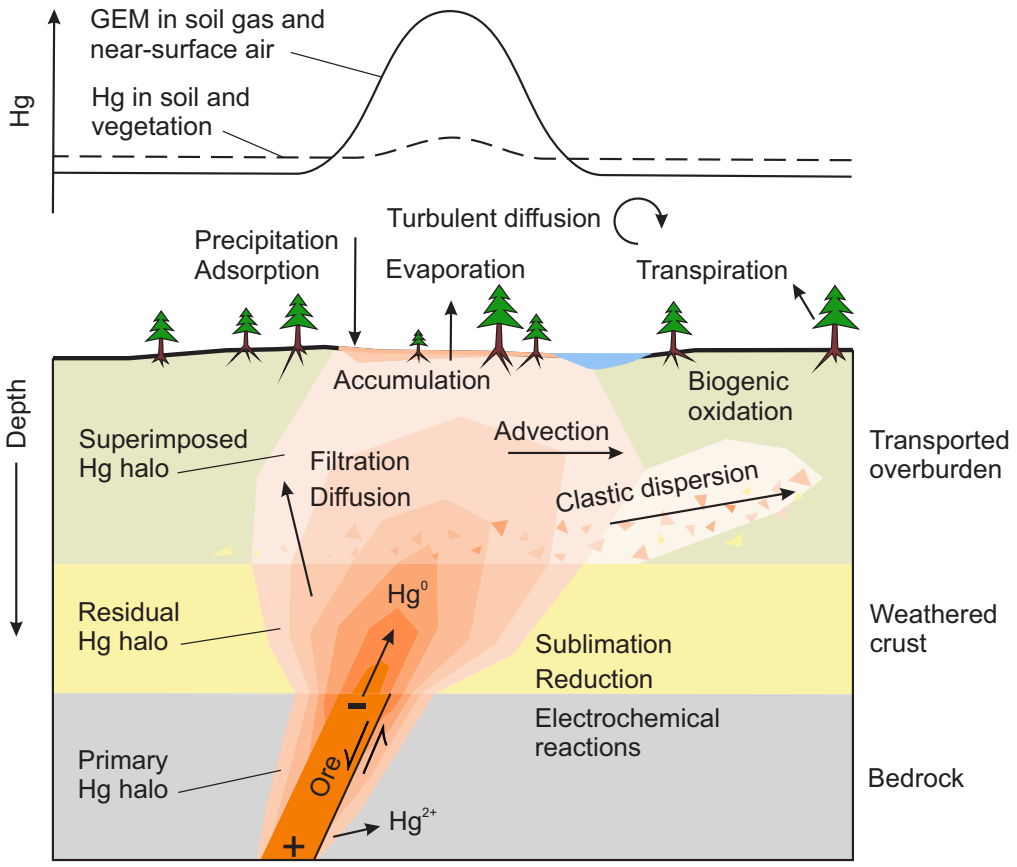

Fig. 11. Model illustrating Hg dispersal from a drift-covered ore deposit and the processes forming gaseous elemental mercury haloes in soil gas, near-surface air and mercury in soil and vegetation. Schematic cross-section showing primary Hg halo of a partly eroded polymetallic ore, residual Hg halo in weathered crust, superimposed Hg halo in a transported overburden, and processes of GEM dispersion and concentration in the surface environment. After Solovov (1985) and Fursov (2006).

Hg emitted into atmosphere is diluted by turbulent diffusion and transferred with air mass movement. Precipitation of atmospheric Hg adsorbed on aerosols and dust leads to Hg accumulation in soil and the hydrosphere. However, if overburden is transported, clastic, hydrochemical, and biochemical dispersion aureoles can be displaced or obscured (Fig. 11).

6. Conclusions

This study follows up on Rukhlov et al. (2021b) with detailed surveys measuring real-time gaseous elemental mercury (GEM) concentrations in air 1 cm above ground across sediment-covered, polymetallic VMS mineralization at the Lara-Coronation occurrence, southern Vancouver Island. New data confirm that direct and continuous analysis using a portable RA-915M Zeeman Hg analyzer can delineate buried mineralization in real-time. Improving on our previous technique, we sampled near-surface air under a bucket to minimize GEM removal and dilution due to wind and turbulent air movement, immediately after disturbing surface materials with a hoe pick. Coupled with more robust signal statistics, the improved technique yielded anomalies up to two orders of magnitude stronger than those reported in Rukhlov et al. (2021b).

To model the release of Hg from mechanically disrupted surface materials, we conducted experiments that measured GEM concentrations in the air of sealed jars containing samples of non-Hg ore minerals before and shortly after shaking. Because GEM levels in shaken jars were up to 122x background Hg, these experiments confirmed the release of weakly adsorbed Hg from overburden sediment and vegetation that were physically disturbed immediately before being sampled.

Our real-time grid survey revealed a pattern of northwest-trending GEM haloes reflecting bedrock structure, including a 224 by 30 m halo above the polymetallic VMS Coronation zone, covered by up to 22 m of overburden. Unrelated to any known mineralization, a prominent GEM halo in the northeast (Fig. 4), that coincides with Hg aureole in soils and vegetation (Fig. 5b), warrants follow-up exploration.

Measuring gaseous mercury using a portable device is simple, effective, and more efficient than standard geochemical surveys that collect sediment, soils, and vegetation. The method will become increasingly useful to the mineral industry as exploration shifts into areas covered by overburden. Future studies should consider porphyry Cu-Mo-Au and epithermal Au-Ag-Cu belts in the province, particularly in the commonly drift-covered Interior Plateau.

Acknowledgments

Lumex Instruments Canada kindly rented out a portable RA-915M Hg analyzer for this study and Mosaic Forest Management kindly granted a permit to access private lands on southern Vancouver Island. We very much appreciate thorough reviews and comments of Professor Elena G. Panova (Institute of Earth Science, Saint-Petersburg State University), and Lawrence B. Aspler (British Columbia Geological Survey).

References cited

Babkin, P.V., Baranov, Yu.E., Vasiliev, V.I., Demidov, N.G., Kirikilitsa, S.I., Kuznetsov, V.A., Nikiforov, N.A., Obolenskiy, A.A., Ozerova, N.A., Smirnov, V.I., Terekhova, G.A., and Fedorchuk, V.P., 1976. Metallogeny of mercury. Nedra, Moscow, 255 p. (in Russian).

Bodnar, M.M., 2017. Modelling geochemical dispersion above a buried polymetallic volcanogenic massive sulphide deposit in a recently glaciated terrain. Unpublished M.Sc. thesis, University of British Columbia, Canada, 212 p.

Cabassi, J., Lazzaroni, M., Giannini, L., Mariottini, D., Nisi, B., Rappuoli, D., and Vaselli, O., 2022. Continuous and near real-time measurements of gaseous elemental mercury (GEM) from an Unmanned Aerial Vehicle: A new approach to investigate the 3D distribution of GEM in the lower atmosphere. Chemosphere 288, 132547. <https://doi.org/10.1016/j.chemosphere.2021.132547>

Fursov, V.Z., 2006. Mercurometric Methods for Geologic Mapping and Ecological Investigations (Methodological Guide). Rosnedra, Geokart, Geos, Moscow, 315 p. (in Russian).

Heberlein, D.R., Dunn, C.E., and Rice, S., 2017. Halogens and other volatile compounds in surface sample media as indicators of mineralization. Part 1: Lara VMS deposit, Vancouver Island, BC (NTS 092B/13). Geoscience BC Report 2017-11, 43 p.

Jeon, B., Cizdziel, J.V., Brewer, J.S., Luke, W.T., Cohen, M.D., Ren, X., and Kelley, P., 2020. Gaseous elemental mercury concentrations along the northern Gulf of Mexico using passive air sampling, with a comparison to active sampling. Atmosphere 11, 1034. <https://doi.org/10.3390/atmos11101034>

Kapusta, J.D., Blackadar, D.W., and McLaughlin, A.D., 1988. 1987 report for drilling conducted on the Lara group I and Lara group II. British Columbia Ministry of Energy, Mines and Petroleum Resources, British Columbia Geological Survey, Assessment Report 17857, 71 p., 7 appendices, scale 1:500 to 1:10,000.

Kelso, I., and Wetherup, S., 2008. Independent technical report and mineral resource estimation: Lara polymetallic property, British Columbia, Canada. NI 43-101 Technical Report, 121 p.

Massey, N.W.D., 1995. Geology and mineral resources of the Duncan sheet, Vancouver Island, 92B/13. British Columbia Ministry of Energy, Mines and Petroleum Resources, British Columbia Geological Survey Paper 1992-4, 124 p.

Massey, N.W.D., Friday, S.J., Tercier, P.E., and Potter, T.E., 1991. Geology of the Duncan area (92B/13). British Columbia Ministry of Energy, Mines and Petroleum Resources, British Columbia Geological Survey Geoscience Map 1991-03, scale 1:50,000.

McLagan, D.S., Mitchell, C.P.J., Huang, H., Lei, Y.D., Cole, A.S., Steffen, A., Hung, H., and Wania, F., 2016. A high-precision passive air sampler for gaseous mercury. Environmental Science & Technology Letters 3, 24-29.

Muller, J.E., 1977. Geology of Vancouver Island. Geological Association of Canada, Mineralogical Association of Canada, Joint Annual Meeting 1977, Field Trip 7, April 21-24, Guidebook, 54 p.

Northcote, K.E., and Muller, J.E., 1972. Volcanism, plutonism, and mineralization: Vancouver Island. Canadian Institute of Mining, Metallurgy and Petroleum, Bulletin 65, 49-57.

Rudnick, R.L., and Gao, S., 2005. Composition of the continental crust. In: Heinrich, D.H., Rudnick, R.L., and Turekian, K.K., (Eds.), The Crust, Treatise on Geochemistry, Volume 3, Elsievier, Amsterdam, pp. 1-64.

Rukhlov, A.S., Mashyanov, N.R., Pitirimov, P.V., Hickin, A.S., Golovetskyy, M., and Coats, B., 2021a. Supplementary data for gaseous elemental mercury (GEM) response from sediment-covered, volcanogenic massive sulphide mineralization on southern Vancouver Island. British Columbia Ministry of Energy, Mines and Low Carbon Innovation, British Columbia Geological Survey GeoFile 2021-15, 1 p.

Rukhlov, A.S., Ootes, L., Hickin, A.S., and Mashyanov, N.R., 2021b. Near-surface mercury vapour haloes in air above ore deposits and faults on Vancouver Island: Insights into buried materials in real-time? In: Geological Fieldwork 2020, British Columbia Ministry of Energy, Mines and Low Carbon Innovation, British Columbia Geological Survey Paper 2021-01, pp. 113-143.

Ruks, T.W., 2015. Stratigraphic and paleotectonic studies of Paleozoic Wrangellia and its contained volcanogenic massive sulfide (VMS) occurrences, Vancouver Island, British Columbia, Canada. Unpublished Ph.D. thesis, University of British Columbia, Canada, 185 p.

Saukov, A.A., Aidinyan, N.K., and Ozerova, N.A., 1972. Studies of Mercury Geochemistry. Nauka, Moscow, 336 p. (in Russian).

Solovov, A.P., 1985. Methods of Geochemical Exploration for Ore Deposits: Textbook. Nedra, Moscow, 294 p. (in Russian).

Sprovieri, F., Pirrone, N., Bencardino, M., D'Amore, F., Carbone, F., Cinnirella, S., Mannarino, V., Landis, M., Ebinghaus, R., Weigelt, A., Brunke, E.-G., Labuschagne, C., Martin, L., Munthe, J., Wängberg, I., Artaxo, P., Morais, F., de Melo Jorge Barbosa, H., Brito, J., Cairns, W., Barbante, C., del Carmen Diéguez, M., Garcia, P. E., Dommergue, A., Angot, H., Magand, O., Skov, H., Horvat, M., Kotnik, J., Read, K.A., Neves, L. M., Gawlik, B. M., Sena, F., Mashyanov, N., Obolkin, V., Wip, D., Feng, X.B., Zhang, H., Fu, X., and Ramachan, R., 2016. Atmospheric mercury concentrations observed at ground-based monitoring sites globally distributed in the framework of the GMOS network. Atmospheric Chemistry and Physics 16, 11915-11935.

Stepanov, I.I., 1997. Mercury-indicator of "hot" hydrothermal zones and dynamic processes accompanied by deformation of rocks. Unpublished D.Sc. thesis, Institute of Mineralogy, Geochemistry and Crystal Chemistry of Rare Elements (IMGRE), Moscow, 165 p. (in Russian).

Sun, X., Si, X., Xiang, Y., and Liu, D., 2017. Soil mercury spatial variations in the fault zone and corresponding influence factors. Terrestrial, Atmospheric and Oceanic Sciences 28, 283-294.

Wetherup, S., 2010. Structural mapping and whole rock geochemical sampling: Lara polymetallic property. British Columbia Ministry of Energy, Mines and Petroleum Resources, British Columbia Geological Survey, Assessment Report 31578, 42 p., 4 appendices, scale 1:20,000.

Yasutake, A., Cheng, J.P., Kiyono, M., Uraguchi, S., Liu, X., Miura, K., Yasuda, Y., and Mashyanov, N.R., 2011. Rapid monitoring of mercury in air from an organic chemical factory in China using a portable mercury analyzer. The Scientific World Journal 11, 1630-1640.

Zherebtsov, Yu.D., Politikov, M.I., and Sikorskiy, V.Yu., 1992. Technology of Mercurometric Prospecting of Ore Deposits. Nedra, Moscow, 176 p. (in Russian).